Stenosis Characterization and Identification for Dialysis Vascular Access

S. Chin[1,2], B. Panda[1-3], M. S. Damaser[2,4] and *S. J. A. Majerus[2,4]*

1. Dept. of Biomedical Engineering, Case Western Reserve University, Cleveland, Ohio, USA
2. Advanced Platform Technology Center, Louis Stokes Cleveland VA Medical Center, Cleveland, Ohio, USA
3. Dept. of Electrical Engineering and Computer Science, Case Western Reserve University, Cleveland, Ohio, USA
4. Dept. of Biomedical Engineering, Lerner Research Institute, Cleveland, Ohio, USA
{slc103, bxp219, sjm18}@case.edu, damasem@ccf.org

Abstract— Vascular access dysfunction is the leading cause of hospitalization for hemodialysis patients and accounts for the most medical costs in this patient population. Vascular access flow is commonly hindered by blood vessel narrowing (stenosis). Current screening methods involving imaging to detect stenosis are too costly for routine use at the point of care. Noninvasive, real-time screening of patients at risk of vascular access dysfunction could potentially identify high-risk patients and reduce the likelihood of emergency surgical interventions. Bruits (sounds produced by turbulent blood flow near stenoses) can be interpreted by skilled clinical staff using conventional stethoscopes. To improve the sensitivity of detection, digital analysis of blood flow sounds (phonoangiograms or PAGs) is a promising approach for classifying vascular access stenosis using non-invasive auditory recordings. Here, we demonstrate auditory and spectral features of PAGs which estimate both the location and degree of stenosis (DOS). Auditory recordings from nine stenosis phantoms with variable DOS and hemodynamic flow rate were obtained using a digital recording stethoscope and analyzed to extract classification features. Autoregressive modeling and discrete wavelet transforms were used for multi-resolution signal decomposition to produce 14 distinct features, most of which were linearly correlated with DOS. Our initial results suggest that the widely-used auditory spectral centroid is a simple way to calculate features which can estimate both the location and severity of vascular access stenosis.

I. INTRODUCTION

Long-term dialysis success and cost is dependent on maintaining a patient's vascular access, a surgically-created artery-vein bypass region that can permit high blood flow and repeated needle sticks. The vascular access is the "Achilles Heel" of hemodialysis, as maintaining the high flow characteristics (access patency) is critical to achieving efficient dialysis treatment. Vascular access dysfunction accounts for most medical costs in dialysis patients [1]. Vascular accesses are routinely monitored to identify internal narrowing (stenosis) which can lead to access blockage (thrombosis). The goal of access monitoring is to pre-emptively treat stenosis with a routine surgical procedure before thrombosis occurs.

Current access monitoring relies on skilled operators and specialized equipment (e.g. imaging) and cannot be used on all patients or at the point of care due to high cost. Commonly used monitoring techniques include surveillance of static dialysis venous pressures, flow monitoring, or duplex ultrasound [2]. Blood flow sounds are occasionally judged by skilled clinical staff during auscultation to determine which patients are at risk of access clotting, and these signals can be easily measured noninvasively at the skin surface. Digital signal analysis of these sounds can produce phonoangiograms (PAGs) which are known to contain specific features that shift in the presence of stenosis. Previous work has determined the classification accuracy of PAGs in pathologic patients, by selectively recording signals from patients with known stenosis severity and location based on conventional imaging [3-5]. Little work has been done to determine how accurately PAGs can detect small changes in stenosis level or determine stenosis location based on recordings at different locations along the blood vessel.

Here, we present an initial analysis of PAG features calculated using multiresolution and autoregressive methods. These features could be used in machine-learning applications, or for simple threshold-based screening purposes. PAGs were recorded in several bench phantoms of vascular stenosis. Phantoms mimicked human anatomy and produced hemoacoustic signals similar to those measured in human patients. Fourteen auditory features were calculated from PAGs and analyzed to determine correlation with stenosis location and severity. Features showed significant covariance, and we determined that the auditory spectral centroid calculated from continuous wavelet transform is promising for both stenosis localization and severity characterization.

II. VASCULAR ACCESS PHANTOM DEVELOPMENT

Because the broad population of hemodialysis patients vary greatly in terms of flow types, flow rates, and degree of stenosis (DOS), a vascular stenosis phantom was developed to mimic human physiology. This phantom allowed independent control of hemodynamic parameters and DOS to reduce the variability in signal analysis to aid feature identification. Phantoms were developed assuming common targets for vascular access in humans: a 6 mm blood vessel, 6 mm vessel diameter, and nominal flow rate of at least 600 mL/min [6]. Vascular stenosis phantoms were made using 6 mm silicone tubing and bio-mimicking silicone rubber (Ecoflex 00-10). A double band suture was tied around the tubing in the center of the phantom to produce turbulent blood flow as predicted by vascular blood flow simulations [7-9]. The DOS was controlled by tying the suture around metal rods with fixed diameters (Fig. 1a). After suturing, liquid silicone rubber was poured around the vessel phantom and the

vessel depth was controlled using a height adjustment jig while the silicone cured (Fig. 1b).
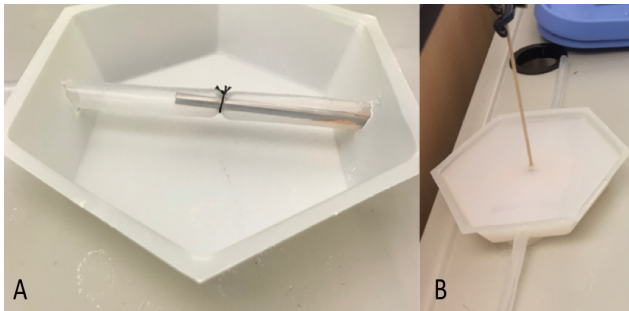
Figure 1. Vascular stenosis phantoms were created using suture bands around silicone tubing (A) and cast into bio-mimicking silicone rubber molds (B).

A. Vascular phantom hemodynamic characterization

Two pulsatile pumps (Cole Parmer MasterFlex L/S, Shurflo 4008) (Fig. 2), were used to create different hemodynamic flows of blood-mimicking fluid through the phantoms at 60 beats per minute [10].

TABLE I. PULSATILE PUMP COMBINATIONS

Flow Number	Flow Type	Flow Rate (mL/min)
1	Monophasic	312
2	Biphasic	97
3	Biphasic	242
4	Biphasic	395
5	Biphasic	404
6	Biphasic	541
7	Biphasic	566
8	Biphasic	695
9	Biphasic	722
10	Biphasic	764
11	Biphasic	843
12	Biphasic	978
13	Biphasic	1002

Thirteen flow types described in Table 1 were used to span the range of flows found in human vascular accesses [11]. Pulsatile pressures and aggregate flow rate were measured with a flow sensor (Omega FMG91-PVDF) and a pressure sensor (PendoTech N-038 PressureMAT). In this study only flows from 500 – 1,010 mL/min were analyzed to represent the nominal flow range in functional vascular accesses [12].
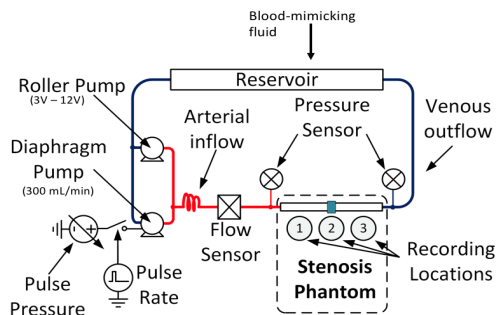
Figure 2. Vascular stenosis phantom flow diagram. The pumping system produced pulsatile flows in a vascular access phantom within physiological ranges of flow and pressure.

III. PHANTOM AUDITORY SIGNAL VALIDATION

10-second PAGs were recorded at three locations on each phantom with a digital recording stethoscope (Littman 3200) and used in signal analysis.
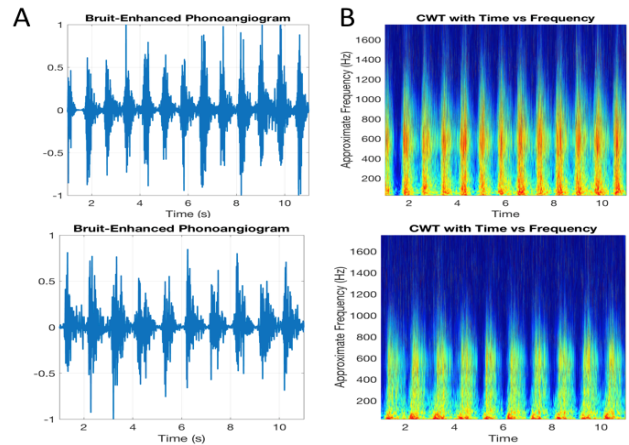
Figure 3. Phonoangiogram (A) and wavelet transform (B) of typical dialysis patient and vascular phantom without stenosis. The phantom produces similar blood flow sounds, but with a more repetitive flow pattern and pulse rate.

Recordings from the vascular phantom were compared to those from humans to ensure that they were physiologically relevant. An aggregate power spectrum was produced from 3,283 unique 10-s recordings obtained from 24 hemodialysis patients over 18 months. Spectral comparisons between human and phantom data were used to reduce time-domain variability e.g. due to heart rate differences (Fig. 3a). Human and phantom spectra followed similar spectral trends and showed similar dynamic range in time-domain analysis (Fig. 3b). Quantitatively, normalized RMS error of the aggregate power spectrum (Fig. 4) was calculated over the aggregate human PAG spectra range. The vascular phantoms matched the aggregate human PAG spectra with a 1.84% normalized RMS error, scaled to the total power spectrum range. This comparison suggested that the vascular stenosis phantoms can adequately replicate PAGs as measured from humans, but with control over vascular access flow rate and stenosis severity.
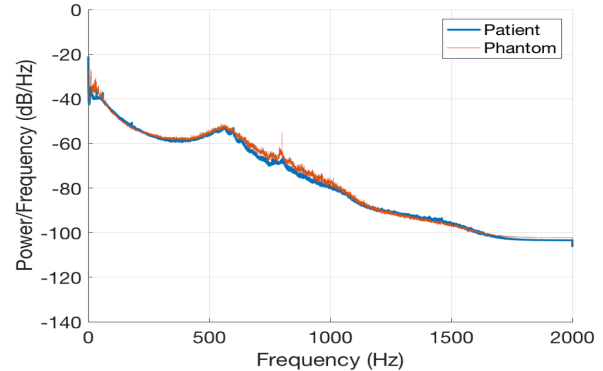
Figure 4. Aggregate power spectrum of patient and phantom PAGs. The spectra varied by about 1.8% RMS, indicating that the phantom reproduces hemoacoustics as recorded from humans.

IV. Phonoangiogram Feature Extraction

Fourteen spectral features were calculated for each PAG (Table II) based partially on previous work [3-5]. All features were calculated in Matlab software based on 10-s PAG recordings from vascular phantoms.

TABLE II. PHONOANGIOGRAM FEATURES

Feature	Feature Description
1	Average of ASC
2	Average of ASF
3	RMS of ASC peaks
4	RMS of ASC peak widths
5	RMS of ASF peak widths
6	RMS of ASC peak prominence
7	RMS of ASF peak prominence
8	Time-aligned ratio of ASC to ASF
9	ASC values at ASF peak
10	Variance of ASC
11	Variance of ASF
12	Covariance of ASC and ASF
13	Correlation corresponding to the covariance matrix of ASC and ASF
14	Standard deviations of the correlation matrix (Feature 13)

Features were derived from two analytical approaches: continuous wavelet transform and autoregressive linear predictive coding [13]. Wavelet coefficients were computed using the Morlet wavelet; wavelet scales were computed over 6 octaves with 12 voices/octave, starting at scale 3. From the wavelet space, the Auditory Spectral Centroid (ASC) was calculated. ASC is the weighted mean of the frequencies present in the signal. The ASC value is calculated using

$$ASC = \frac{\sum_{n=0}^{N-1} f(n)x(n)}{\sum_{n=0}^{N-1} x(n)}, \tag{1}$$

where $x(n)$ is the weighted frequency value of bin number n, and $f(n)$ is the center frequency of bin number n [14].

Autoregressive modeling was used to produce an analytic signal similar to a Hilbert envelope, but derived from the discrete cosine transform. By fitting a linear predictive model to the frequency dual of the PAG, a smooth approximation of the time-domain power envelope was obtained. This analytical envelope is highly correlated to a common measure, Auditory Spectral Flux (ASF), which describes how quickly the power spectrum of a signal is changing. Because the modeled analytical envelope was smoother, it was used as a surrogate for ASF in feature extraction.

Seven features were derived from the ASC and ASF equivalent signals: mean value, rms value of ASC peaks, rms value of ASC and ASF peak widths, and rms value of ASC and ASF peak prominence. Seven multi-variate features were also calculated: correlation and covariance between ASC and ASF, the time-aligned ratio of ASC to ASF, and the corresponding ASC value at ASF peaks.

A. Stenosis feature correlation plots

Qualitative analysis of each computed feature was performed using heat maps for each stenosis phantom, combining variability in recording location and hemodynamic flow rate. All maps showed feature trends dependent on flow type and recording location. Of the 14 features, the mean ASC value showed the clearest trend at the site of stenosis across the different phantoms (Fig. 5).
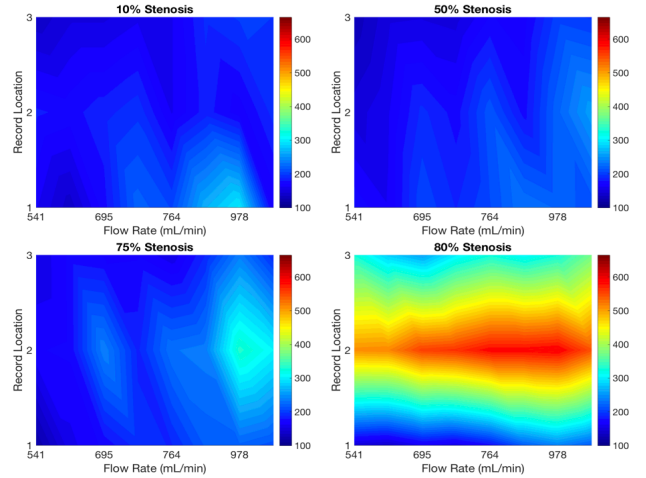
Figure 5. ASC values at different flow types and recording locations for phantoms with DOS between 10 – 80%.
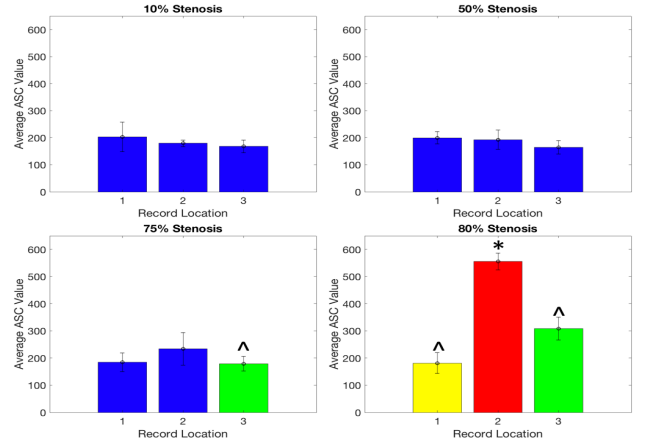
Figure 6. Average ASC value across physiologic flow levels at all three recording locations for phantoms with DOS between 10 – 80%. ^ p<0.05 for Location 1 and Location 2 or Location 2 and Location 3. * p<0.05 for all three locations.

Because mean ASC value correlated strongly with DOS, here we describe its performance at localizing and describing stenosis level. Many of the analyzed features, however, produce similar outcomes. To mimic a clinical monitoring scenario, in which patient blood flow rate varies according to anatomical and physiologic factors, all observations at a flow rate greater than 500 mL/min were pooled for statistical analysis. Paired t-test comparisons were used to determine statistical significance between mean ASC values at each recording site and for each stenosis phantom (Fig. 6).

ASC values across the three recording locations were not statistically significant at lower DOS (below 50%). At 60% DOS, a statistically-detectable shift between recording locations first became apparent (p = 0.0018). Above 80% DOS, ASC values at all recording locations were statistically distinct (p = 2.37e-09). The differentiation of the average ASC value at each location suggests that signal processing of PAGs can be used to localize vascular stenosis.

To determine how well mean ASC value can describe the level of stenosis, recordings from only Location 2 for each phantom were analyzed (Fig. 7). Beginning with a DOS at 60%, a monotonic increase in mean ASC value was observed as the DOS increases. Specifically, the mean ASC value increased from 169.83 ± 24.48 Hz at 60% stenosis to 555.92 ± 31.21 Hz at 80% stenosis. This nonlinear trend implies that the ASC can estimate DOS with increasing specificity above 60% stenosis.
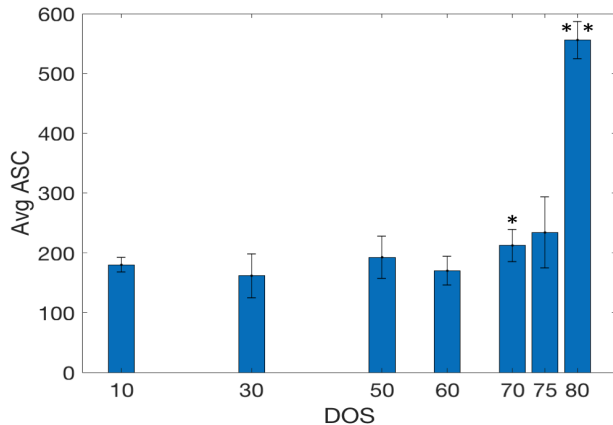
Figure 7. Mean ASC values for all flow types recorded at Location 2 for each phantom. A statistically-significant shift was observed for each phantom above 60%. Phantoms below 60% showed no discernible trend in mean ASC value.

V. Discussion & Conclusion

Because PAGs are recorded noninvasively with a stethoscope, they have the potential to be used for stenosis risk assessment even in asymptomatic patients. In this limited study, we developed vascular access phantoms which produced hemoacoustic signals to mimic those measured in humans. One limitation of the phantoms, however, was the fixed geometry (6mm blood vessel, 6mm below skin surface). Actual vascular access anatomy varies widely, especially over years of vascular remodeling, and our phantoms did not account for vessel bends, pseudo-aneurysms, or other morphological structures. A second limitation is that the phantoms required significantly larger systolic blood pressures (up to 350 mmHg) to support flow levels above 500 mL/min with DOS 80% and above. Vascular remodeling which occurs in humans to accommodate sustained high blood pressures would limit pressure increase due to stenosis [15]. However, the vascular stenosis phantom is not capable of remodeling and therefore does not adapt to stenosis. Due to these limitations, we did not take blood pressure into account when defining the physiologically relevant flow types.

Overall, our results suggest that the mean ASC parameter alone can estimate both the location and degree of stenosis for DOS above 70% (Fig. 7). One key finding was that ASC showed a clear increase for recordings made very close to the actual stenosis location. This is likely due to turbulent flow which is prominent in the area just distal to the lesion [16]. A second finding was that ASC was monotonically correlated with DOS above 60%, but showed little variation prior to the level. This is likely due to the well-known phenomena in which stenosis only becomes hemodynamically significant starting at 50% [3]. Considering this effect, ASC showed a

statistically-significant increase for each tested stenosis above 50%. Future steps will be to investigate whether the ASC of patient data is correlated to clinically-confirmed levels of stenosis.

References

[1] H. I. Feldman, S. Kobrin and A. Wasserstein, "Hemodialysis Vascular Access Morbidity," *Journal of the American Society of Nephrology,* vol. 7, pp. 523-535, 1996.

[2] M. Allon and M. L. Robbin, "Hemodialysis vascular access monitoring: current concepts," *Hemodialysis international,* vol. 13, no. 2, pp. 153-162, 2009.

[3] P. Sung, C. Kan, W. Chen, L. Jang and J. Wang, "Hemodialysis vascular access stenosis detection using auditory spectro-temporal features of phonoangiography," *Med Biol Eng Comput,* vol. 53, pp. 393-403, 2015.

[4] Y.-C. Du, W.-L. Chen, C.-H. Lin, C.-D. Kan and M.-J. Wu, "Residual Stenosis Estimation of Arteriovenous Grafts Using a Dual-Channel Phonoangiography With Fractional-Order Features," *IEEE Journal of Biomedical and Health Informatics,* vol. 19, no. 2, pp. 590-600, 2015.

[5] Y.-C. Du, C.-D. Kan, W.-L. Chen and C.-H. Lin, "Estimating Residual Stenosis for an Arteriovenous Shunt Using a Flexible Fuzzy Classifier," *Computing in Science & Engineering,* vol. 16, no. 6, pp. 80-91, 2014.

[6] D. R. Hassell, F. M. van der Sande, J. P. Kooman, J. P. Tordoir and K. M. leunissen, "Optimizing dialysis dose by increasing blood flow rate in patients with reduced vascular-access flow rate," *American Journal of Kidney Diseases,* vol. 38, no. 5, pp. 948-955, 2001.

[7] H. Mansy, S. Hoxie, N. Patel and R. Sandler, "Computerised analysis of auscultatory sounds associated with vascular patency of haemodialysis access," *Medical & Biological Engineering & Computing,* vol. 43, pp. 56-62, 2005.

[8] Y. M. Akay, M. Akay, W. Welkowitz, J. L. Semmlow and J. B. Kostis, "Noninvasive acoustical detection of coronary artery disease: a comparitive study of signal processing methods," *IEEE Transactions on Biomedical Engineering,* vol. 40, no. 6, p. 1993, 571-578.

[9] D. W. Pravica, M. Bier and O. Day, "Murmurs and noise caused by arterial narrowing - Theory and clinical practice," *Fluctuation and Noise Letters,* vol. 6, no. 4, pp. 415-25, 2006.

[10] J. E. Hall, "The Normal Electrocardiogram," in *Guyton and Hall Textbook of Medical Physiology*, Jackson, Elsevier, Inc., 2016, pp. 131-137.

[11] E. Wijnen, X. H. Keuter, N. R. Planken, F. M. Van Der Sande, J. H. Tordoir, K. M. Leunissen and J. P. Kooman, "The Relation Between Vascular Access Flow and Different Types of Vascular Access With Systemic Hemodynamics in Hemodialysis Patients," *Artificial Organs,* vol. 29, no. 12, pp. 960-964, 2005.

[12] K. Jindal, C. T. Chan, C. Deziel, D. Hirsch, S. D. Soroka, M. Tonelli and B. F. Culleton, "Vascular Access," *Journal of the American Society of Nephrology,* vol. 17, no. 3, pp. 16-23, 2006.

[13] S. Majerus, T. Knauss, S. Mandal, G. Vince and M. Damaser, "Bruit-enhancing phonoangiogram filter using sub-band autoregressive linear predictive coding," in *2018 Engineering in Medicine and Biology Conference*, Honolulu, 2018.

[14] G. Peeters, A large set of audio features for sound description, Paris: IRCAM, 2004.

[15] J. E. Hall, "Local and Humoral Control of Tissue Blood Flow," in *Guyton and Hall Textbook of Medical Physiology*, Philadelphia, Elsevier, 2016, pp. 203-214.

[16] M. Jahangiri, M. Saghafian and M. R. Sadeghi, "Numerical Study of Turbulent Pulsatile Blood Flow Through Stenosed Artery Using Fluid-Solid Interaction," *Computational and Mathematical Methods in Medicine,* vol. 2015, 2015.